Blocker State Dependence and Trapping in Hyperpolarization-activated Cation Channels: Evidence for an Intracellular Activation Gate

Ki Soon Shin, Brad S. Rothberg, and Gary Yellen

From the Department of Neurobiology, Harvard Medical School, 220 Longwood Avenue, Boston, Massachusetts 02115

ABSTRACT Hyperpolarization-activated cation currents (I_h) are key determinants of repetitive electrical activity in heart and nerve cells. The bradycardic agent ZD7288 is a selective blocker of these currents. We studied the mechanism for ZD7288 blockade of cloned I_h channels in excised inside-out patches. ZD7288 blockade of the mammalian mHCN1 channel appeared to require opening of the channel, but strong hyperpolarization disfavored blockade. The steepness of this voltage-dependent effect (an apparent valence of ~4) makes it unlikely to arise solely from a direct effect of voltage on blocker binding. Instead, it probably indicates a differential affinity of the blocker for different channel conformations. Similar properties were seen for ZD7288 blockade of the sea urchin homologue of I_h channels (SPIH), but some of the blockade was irreversible. To explore the molecular basis for the difference in reversibility, we constructed chimeric channels from mHCN1 and SPIH and localized the structural determinant for the reversibility to three residues in the S6 region likely to line the pore. Using a triple point mutant in S6, we also revealed the trapping of ZD7288 by the closing of the channel. Overall, the observations led us to hypothesize that the residues responsible for ZD7288 block of I_h channels are located in the pore lining, and are guarded by an intracellular activation gate of the channel.

KEY WORDS: mHCN1 • SPIH • ZD7288 • pore

INTRODUCTION

Hyperpolarization-activated nonselective cation current (I_h)[1] was first described in sinoatrial node cells of the heart, and is thought to play an important role in producing the pacemaker potential that controls the beating rate of the heart (Brown et al., 1979; Brown and DiFrancesco, 1980; Yanagihara and Irisawa, 1980; DiFrancesco, 1986; for review see DiFrancesco, 1993). Subsequently, I_h has been identified in Purkinje fibers (DiFrancesco, 1981), atrial and ventricular muscle (Yu et al., 1993), and in both peripheral (Mayer and Westbrook, 1983) and central neurons (for review see Pape, 1996). Because I_h is a mixed inward Na^+/K^+ current with an equilibrium potential of about −30 mV, it causes a slow depolarization leading to the threshold for action potential generation. The current is also modulated by direct action of cAMP (DiFrancesco and Tortora, 1991). I_h can control rhythmic firing in thalamic relay neurons (Pape and McCormick, 1989; McCormick and Bal, 1997; Luthi et al., 1998) and hippocampal interneurons (Maccaferri and McBain, 1996; Strata et al., 1997).

Many years of effort to identify the molecular nature of I_h currents have revealed a gene family that encodes I_h channels. They turned out to be related both to voltage-gated K^+ channels and to cyclic nucleotide–gated channels. The first member of the gene family encoding the I_h channel was mBCNG1 (now termed mHCN1; Santoro et al., 1998). Heterologous expression in *Xenopus* oocytes demonstrated that mHCN1 forms a hyperpolarization-activated channel that was weakly selective for K^+ over Na^+ and was blocked by external Cs^+. So far, four members of the HCN gene family (HCN1, HCN2, HCN3, and HCN4) have been identified in mammals (Santoro et al., 1997; Ludwig et al., 1998, 1999; Santoro et al., 1998; Ishii et al., 1999; Seifert et al., 1999). Of the four cloned genes, three genes have been heterologously expressed. They generated hyperpolarization-activated currents with distinct properties. HCN1 channels activate relatively rapidly on hyperpolarization and show little cAMP effect, whereas HCN2 channels activate more slowly and show a strong cAMP effect. HCN4 channels are similar to HCN2, but they activate even more slowly. In situ hybridization experiments showed different regional expression of HCN isoforms (Santoro et al., 2000), suggesting that HCN isoforms with distinct biophysical characteristics play specific functional roles in specific regions.

Because I_h current contributes to the pacemaker potential in the heart sinoatrial node cells, drugs that inhibit I_h channels may be therapeutically useful in the treatment of certain cardiac arrhythmias and ischemic heart disease. The drug ZD7288 is a bradycardic agent

Address correspondence to Dr. Gary Yellen, Department of Neurobiology, Harvard Medical School, 220 Longwood Avenue, Boston, MA 02115. Fax. (617) 432-0121; E-mail. gary_yellen@hms.harvard.edu

[1]*Abbreviations used in this paper:* 4-AP, 4-aminopyridine; I_h, hyperpolarization-activated nonselective cation current.

J. Gen. Physiol. © The Rockefeller University Press • 0022-1295/2001/02/91/11 $5.00
Volume 117 February 2001 91–101
http://www.jgp.org/cgi/content/full/117/2/91

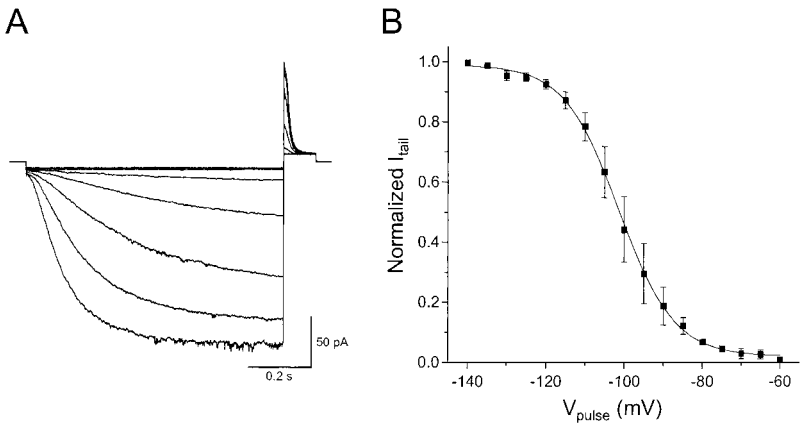

FIGURE 1. Hyperpolarization-activated mHCN1 currents. (A) Representative recordings from inside-out patches excised from HEK293 cells expressing mHCN1. Currents were elicited by an 800-ms hyperpolarization from a holding voltage of +10 mV to voltages ranging from −140 to −60 mV in 10-mV increments. Voltage was returned to +30 mV for 150 ms to measure the tail currents. (B) Voltage dependence of channel activation. Initial tail current amplitudes at +30 mV (as shown in A) were normalized to the maximal tail current. Solid line shows the best fit of the data to a Boltzmann function; normalized current = $1/[1 + \exp((V_{1/2} - V)/\text{slope})]$, where V is voltage in millivolts and $V_{1/2}$ is the activation midpoint voltage. A mean $V_{1/2}$ of −101.3 mV and a slope of e-fold change for 7.1 mV were determined from five experiments.

that selectively blocks the cardiac pacemaker current, I_f (BoSmith et al., 1993). This drug also blocks I_h in guinea pig substantia nigra neurons, rat hippocampal CA1 cells, cat ventrobasal thalamocortical neurons, and bullfrog photoreceptors, with minor effects on other membrane properties (Harris and Constanti, 1995; Gasparini and DiFrancesco, 1997; Williams et al., 1997; Satoh and Yamada, 2000). In the present study, we tried to elucidate the precise molecular mechanism for ZD7288 blockade. We found that ZD7288 blocked mHCN1 channels only after they were opened by hyperpolarization. Further hyperpolarization reduced blockade sharply, with an apparent valence ($z\delta$) of ~4, which was higher than expected for a direct effect of voltage on the blocker. We suspect that this voltage dependence arises from preferential binding to certain conformations visited during voltage-dependent gating. We also tested the effect of ZD7288 on SPIH, a channel cloned from sea urchin testis with characteristics similar to mammalian I_h channels (Gauss et al., 1998). Blockade of SPIH also required the opening of the channel, but in contrast to the mHCN1 effects, this blockade was partially irreversible. To explore the molecular basis for the difference in the reversibility of ZD7288 block, we constructed chimeric channels from mHCN1 and SPIH and localized the structural determinant for reversibility to the S6 region. Specifically, three amino acid differences in the pore-lining S6 region appeared to be critical for the reversibility of blocker binding. Using a triple mutant, we found that ZD7288 can be trapped by the closing of the channel. Based on these results, we propose that ZD7288 blocks the pore of I_h channels at a site guarded by an intracellular activation gate of the channel.

TABLE I

Structure of Chimeras between mHCN1 and SPIH

Clone or chimera name	Sequence description
mHCN1	h M_1-N_{909}
H-S/P	h M_1-Q_{312}, s E_{394}-L_{767}
H-S/S5	h M_1-S_{282}, s A_{364}-S_{469}, h L_{384}-N_{909}
mHCN1-χ3	Y355F, M357L, V359I in mHCN1
SPIH-χ3	F456Y, L458M, I460V in SPIH
SPIH	s M_1-L_{767}

MATERIALS AND METHODS

Expression of Recombinant I_h Channels

For channel expression, we used the mHCN1 channel (Santoro et al., 1998) and SPIH channel (Gauss et al., 1998). We found that a point mutation in the S4 region of SPIH (M349I) increased the expression of the channel. This mutation shifted the conductance–voltage (G-V) relation to the left by ~10 mV without changing any other gating properties. The shift probably reduces the number of open I_h channels in the transfected cells in culture: open I_h channels appear to kill the cultured cells. Therefore, we used this mutant as a wild-type SPIH channel throughout the experiments. The channel cDNA was subcloned into the GW1-CMV expression vector (British Biotechnology). Human embryonic kidney 293 cells (HEK 293; American Type Culture Collection) were transiently transfected with expression plasmid containing mHCN1 or SPIH cDNA (40 μg in 200-μl cell suspension) using electroporation. The channel expression plasmid was cotransfected with the πH3-CD8 plasmid (Seed and Aruffo, 1987), which expresses the α subunit of the human CD8 lymphocyte antigen. Cells expressing the CD8 antigen were identified visually by decoration with antibody-coated beads (Jurman et al., 1994).

Construction of Chimeras and Site-directed Mutagenesis

Several chimeras were constructed between mHCN1 and SPIH channels using native or introduced enzyme sites. The nucleotide sequences of the chimeras were verified by sequencing. The structures of the chimeras are shown in Table I. Point mutations were introduced by PCR (Ausubel et al., 1996) and confirmed by sequencing.

Solutions and Electrophysiological Recordings

All experiments were done with excised inside-out patches (Hamill et al., 1981) from identified transfected cells 1–2 d after transfection. The methods for electrophysiological recordings

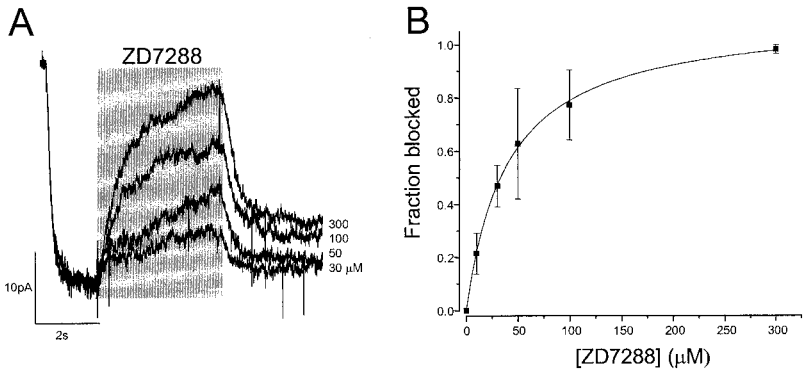

FIGURE 2. Concentration dependence of ZD7288 blockade of mHCN1 currents. (A) Superimposed current records at −110 mV with different ZD7288 concentrations. ZD7288 was applied for 4 s, as indicated by the shaded bar. (B) Fractional blockade of mHCN1 at −110 mV versus ZD7288 concentration. The solid line is the best fit with the equation $f = [ZD]/([ZD] + K_d)$. The fitted K_d was 40.5 ± 3.3 μM (data points with $n = 3–5$).

and rapid perfusion switches have been described previously (Liu et al., 1997). Both internal and external solutions contained the following: 160 mM KCl, 0.5 mM $MgCl_2$, 1 mM EGTA, and 10 mM HEPES, pH 7.4. ZD7288 (Tocris) was dissolved in distilled water to make a 20-mM stock solution that was stored at −20°C. An aliquot was diluted into the internal solution to obtain the desired final concentration.

RESULTS

Block of mHCN1 by ZD7288

mHCN1 channels were expressed in HEK293 cells at levels sufficient to permit recording of currents from excised inside-out patches (Fig. 1 A). The channels showed slow activation (hundreds of milliseconds) upon hyperpolarization. The G-V relationship was determined by measuring the initial tail currents at +30 mV after steps to various voltages. Fitting a Boltzmann function (Fig. 1 B) gave an approximate midpoint voltage ($V_{1/2}$) of −101 mV and slope of e-fold/7.1 mV, corresponding to an effective gating valence (zδ) of ∼3.6. These properties are similar to those originally reported for this clone expressed in *Xenopus* oocytes ($V_{1/2}$ = −99.9 mV, slope = 6.0 mV; Santoro et al., 1998). We could not find any clear evidence for a cAMP effect on mHCN1 (data not shown).

We tested the effect of various concentrations of ZD7288 on mHCN1 channels at a single voltage (Fig. 2 A). The blocker was applied to the exposed intracellular face of inside-out patches for 4 s, after the channels were fully opened at −110 mV (Fig. 2 A). The current was reversibly blocked in a dose-dependent manner. Most of the current recovered within 1 s. Although there was a also slow component of recovery (>5 s), complete recovery was achieved between trials using a series of four 800-ms step pulses to −140 mV. The fraction of blocked current measured at the end of each application is plotted in Fig. 2 B. The data were fitted with a K_d of ∼41 μM.[2] When the blocker was applied instead to the extracellular side of the channels, it took a long time (in minutes) to get the blocking effect (data not shown), indicating that the block occurs from the intracellular side of the channels, as previously suspected from whole-cell studies (BoSmith et al., 1993; Harris and Constanti, 1995; Gasparini and DiFrancesco, 1997; Luthi et al., 1998; Satoh and Yamada, 2000).

Block of mHCN1 Is Voltage-dependent and Requires Channel Opening

The blocking effect of ZD7288 on mHCN1 had a surprisingly strong voltage dependence (Fig. 3, A and B). The channels could be blocked effectively at voltages producing low levels of activation (−90 and −100 mV), but the blockade was reduced at more negative voltages, at which the channels were fully opened. To quantify this voltage dependence, the fraction blocked was fitted by a Boltzmann equation. (In this case, failure to achieve complete equilibration may lead us to overestimate the limiting degree of relief of blockade at negative voltages, or to overestimate the steepness of the voltage effect, or both.) The effective valence value (zδ) derived from the steepness was 4.2, which was a value comparable to that for gating of mHCN1 (3.6) obtained from the G-V. This very high zδ value cannot be explained by the intrinsic voltage dependence of ZD7288, whose charge is +1. Instead, the steep voltage dependence might be related to the gating of the channels. In particular, it seemed plausible that the steep voltage dependence was due to preferential closed state blockade.

Earlier experiments on I_h in cardiomyocytes and neurons showed some relief of block on hyperpolarization (BoSmith et al., 1993; Harris and Constanti, 1995; Gasparini and DiFrancesco, 1997), and these studies also suggested that blockade is non–use-dependent and does not require opening of channels. However, we found that the rapid blockade of mHCN1 does require channel opening. We tested this by applying blocker briefly to either closed or open channels. Relying on the slow recovery from the block, we applied another activating pulse to test whether the blocker had bound

[2]The failure of the blockade to reach steady state, because of the slow second phase of blockade, means that the measured dissociation constant reported here is an upper limit and the true affinity for long applications may be higher.

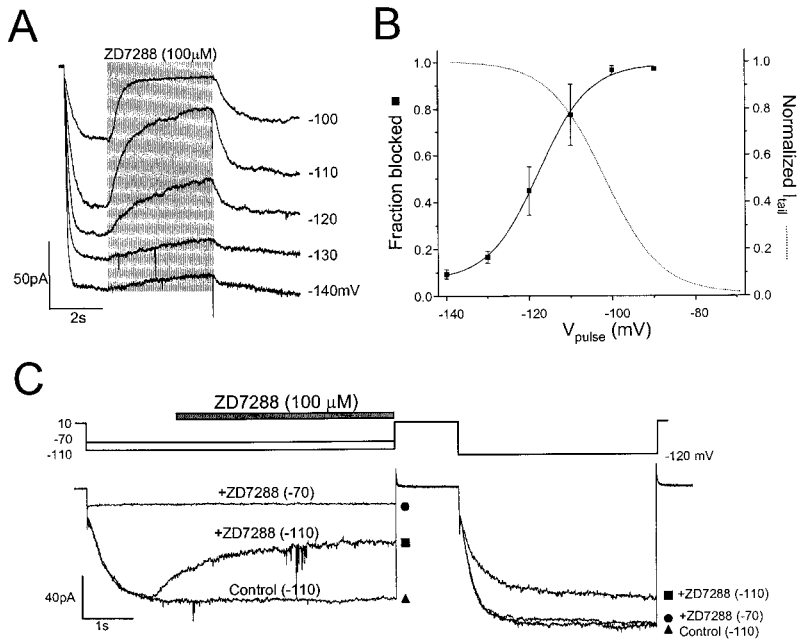

FIGURE 3. Voltage-dependent and open channel block of mHCN1 current. (A) Superimposed current record from −140 to −90 mV with 100 μM ZD7288. ZD7288 was applied for 4 s, as indicated by the shaded bar. (B) Fractional block with 100 μM ZD7288 measured at different voltages. The data were fitted with a Boltzmann equation with a $V_{1/2}$ of −117.5 mV and zδ of 4.2 (n = 3–5). The dotted line shows the G-V of mHCN1 for comparison. (C) Open channel block of mHCN1 by ZD7288. ZD7288 (100 μM) was applied for 4 s at −70 or −110 mV during the period indicated by the bar, and the voltage was returned to +10 mV for 1 s to close the channels. Finally, a second activating pulse at −120 mV was applied to test the remaining blockade of the channel. For the control, the voltage step was applied without blocker present.

during the previous application (Fig. 3 C). When blocker was applied during an activating pulse to −110 mV, the second pulse was noticeably reduced compared with the control. (Full recovery was seen later after pulsing to −140 mV.) However, application of blocker at −70 mV, when the channels were closed, produced no such reduction in the second pulse. Thus, for brief applications, ZD7288 blockade of mHCN1 requires channel opening.

ZD7288 Blockade of SPIH

The sea urchin I_h channel (SPIH) was also expressed by transfection in HEK293 cells (Fig. 4 A). SPIH showed rapid inactivation at hyperpolarized voltages. Intracellular application of cAMP (100 μM) removed this inactivation and increased the peak current level by ∼10-fold. Fig. 4 B shows the voltage dependence of the relative open probability of SPIH channels in the presence of cAMP. The characteristics are quite comparable to the properties originally reported for this clone with excised inside-out patches (Gauss et al., 1998).

ZD7288 readily blocked the SPIH channels (Fig. 5 A). (Unless otherwise indicated, further experiments with SPIH were done in the presence of 100 μM cAMP to produce maximal activation of the channels.) Some fraction of the current recovered rapidly from the blockade, but a portion was irreversibly blocked and did not recover, even with prolonged hyperpolarization to −160 mV (data not shown).

We determined the rate of onset of irreversible blockade at different voltages, by tracking the current during a series of brief applications (Fig. 5 B). The dots indicate the current during monitoring pulses applied every 4 s; at each arrow, ZD7288 was applied for 1 s during an activating pulse (inset), in this case to −110 mV. After each application, there was a step reduction in

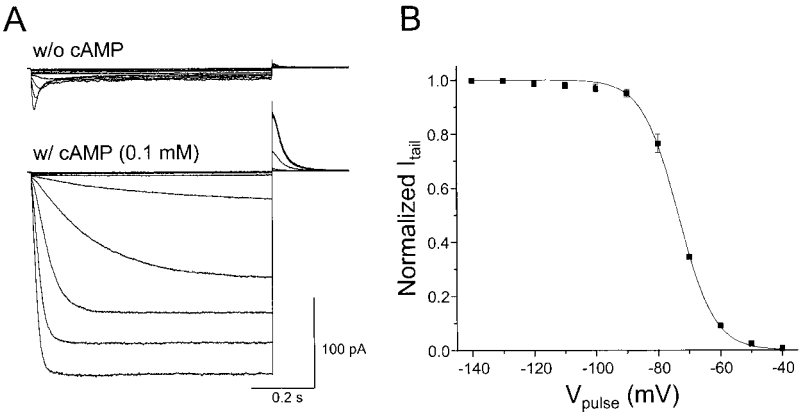

FIGURE 4. Hyperpolarization-activated SPIH currents. (A) Recordings of SPIH currents in the presence or absence of cAMP. Currents were measured with excised inside-out patches from SPIH-expressing HEK293 cells in the presence or absence of cAMP (100 μM). Currents were elicited by a series of 800-ms hyperpolarizing voltage steps between −120 and −30 mV in 10-mV steps from a holding voltage of +10 mV. (B) Voltage dependence of channel activation. Tail current amplitudes at +30 mV in the presence of 100 μM cAMP (as shown in A) were normalized to the maximal tail current. The solid line shows the Boltzmann fit to the data with a mean midpoint voltage $V_{1/2}$ of −73.5 mV and a slope of e-fold change for 5.4 mV (each point is the mean of five experiments).

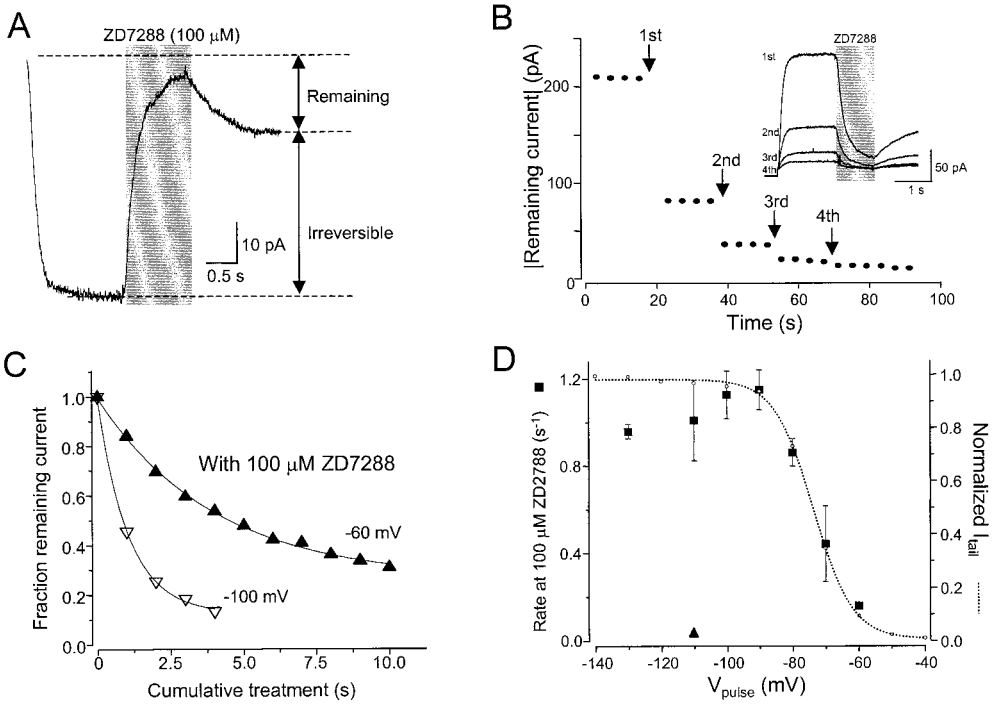

FIGURE 5. ZD7288 block of SPIH. (A) ZD7288 (100 μM) was applied to an excised inside-out patch for 1 s at −110 mV. Much of the current did not recover after removal of the blocker. (B)100 μM ZD7288 was repeatedly applied for 1 s at −110 mV at each time point (arrows). The inset shows the superimposed traces of each application. The traces are flipped over to show the reduction in the size of current because of the irreversible blockade by ZD7288. Dots indicate the steady-state current in response to an activating voltage step to −120 mV applied every 4 s between blocker applications. (C) Fractional remaining currents after application of ZD7288 (100 μM) were measured (as shown in B) and plotted against cumulative treatment time. The rate constant for the irreversible block was calculated from a time constant of a monoexponential fit to the data. In the same way, the rates at different voltages were determined. (D) Rate of irreversible block in SPIH. The rates were measured at different voltages (as described in B and C) in the presence of cAMP (square). The triangle indicates the rate of irreversible block at −110 mV in the absence of cAMP. For comparison, the normalized G-V relationship of SPIH is shown as open circles. All individual points give the mean and SEM of at least three determinations.

the size of the current, and the current remaining after each application was plotted to determine the rate constant of irreversible blockade (Fig. 5 C). Rates of irreversible blockade determined at different voltages varied in parallel with the G-V of SPIH (Fig. 5 D), implying that this process requires channel opening. In the absence of cAMP, the rate was >20 times slower than that with cAMP (Fig. 5 D, triangle). This too supports the idea that ZD7288 can reach its binding site only in the open state of the channels. As seen for the reversible blockade of mHCN1, there was also some reduction of blockade at the most negative voltages.

The S6 Region Is Responsible for Irreversible ZD7288 Block

mHCN1 and SPIH showed different reversibility of ZD7288 blockade, as shown by the simple comparison at the top of Fig. 6. Whereas the blockade of mHCN1 recovered fully during the series of 800-ms voltage steps to −140 mV, SPIH exhibited irreversible blocker binding. After each application to SPIH, there was a step reduction in current level, and the reduction was not recovered with the series of steady pulses to –140 mV. To explore the molecular basis for this difference in the reversibility of ZD7288 blockade, we constructed chimeric channels from mHCN1 and SPIH. If a transplanted region conferred the blockade properties of the donor, then this region might be important for the binding of ZD7288. Because ZD7288 appears to act on open channels, we examined the role of the S5, P, and S6 regions, which form the pore domain. As shown in Fig. 6, transplanting a relatively small portion of SPIH into the mHCN1 background was sufficient to produce irreversible binding of ZD7288 (H-S/P and H-S/S5). Because both chimeras shared the S6 region of SPIH, we focused our attention on this region.

Three Residues in the S6 Region Are Critical for Irreversible ZD7288 Blockade

To pinpoint the residues responsible for the reversibility, we compared the amino acid sequences of SPIH and mHCN1 (Fig. 7). Overall, they showed high homology. In the lower part of S6, which is expected to contribute to the cytoplasmic entrance to the pore, three amino acids are different: residues Y355, M357, and V359 in mHCN1 correspond to F456, L458, and I460 in SPIH. Therefore, we focused on these residues as candidates for determining the reversibility of the blocker effect. Our study of the mutants at these residues was limited by the fact that not all combinations yielded functional expression. In fact, only triple mutants gave good measurable currents.

We examined the effect of ZD7288 on mutant mHCN1-χ3, which had the three SPIH residues substituted in the mHCN1 background (F, L, and I replacing

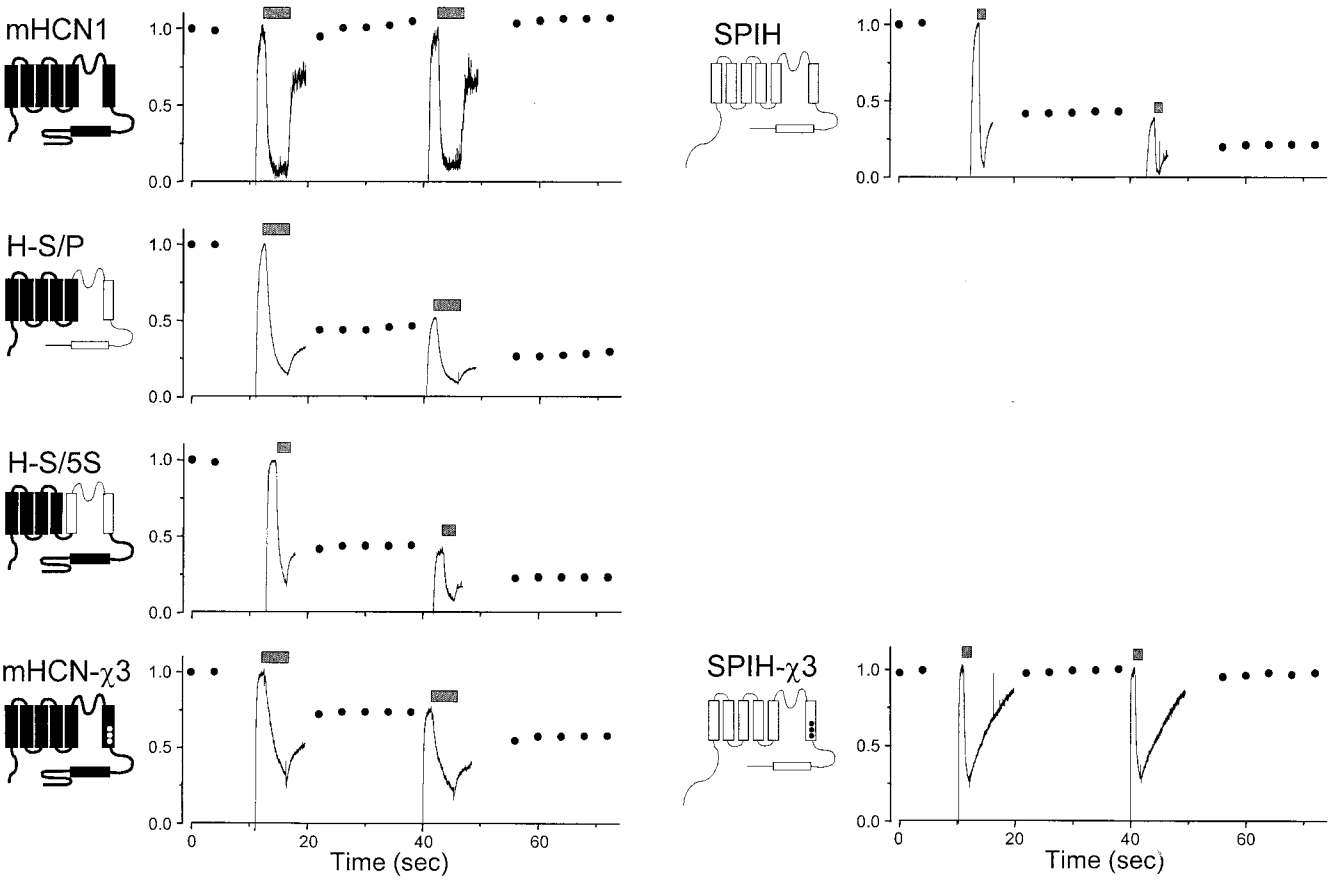

FIGURE 6. Reversibility of ZD7288 blockade in different chimeras. 100 μM ZD7288 was repeatedly applied at −110 mV at each time point indicated by the bars (4 s for mHCN1, H-S/P, and mHCN1-χ3; 2 s for H-S/S5; and 1 s for SPIH and SPIH-χ3). Between the applications, 800 ms-long activating voltage steps to −140 mV were applied every 4 s, and the steady-state currents were measured. Dots indicate normalized currents to the maximal steady-state current level. The maximal currents at −140 mV were as follows: −30.2 pA for mHCN1; −526 pA for H-S/P; −650 pA for H-S/S5; −98.2 pA for mHCN1-χ3; −85 pA for SPIH; and −78.2 pA for SPIH-χ3. The current traces were also normalized to the maximal current level measured just before the first blocker application. Schematic representations of chimeras are shown to the left of each graph.

Y, M, and V). Remarkably, this triple mutant of mHCN1 showed irreversible blockade comparable to that for SPIH itself (Fig. 6, bottom left). Therefore, we next studied the inverse mutant, with the three mHCN1 residues substituted into the SPIH background (F456Y, L458M, and I460V; named SPIH-χ3). Surprisingly, the triple mutations in SPIH resulted in a completely reversible blockade (Fig. 6, bottom right). These results imply that the three residues in SPIH are critical for the irreversible blocker binding. These mutations did not produce drastic changes in the gating parameters of the channels (Table II), arguing against an indirect effect on blockade through altered gating.

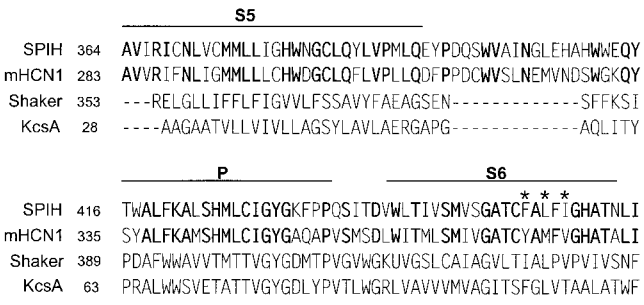

FIGURE 7. Sequence alignment of the S5, P, and S6 regions. Amino acids that are identical between SPIH and mHCN1 are shown in bold. The three residues in the S6 region that are different from each other and appear to be critical in the reversibility of ZD7288 blockade are indicated by asterisks.

Trapping of ZD7288 in the SPIH-χ3 Mutant

Our earlier results suggested that blocker might be bound preferentially to closed channels, but that blocker could not enter closed channels. The clear prediction is that blocker should also be unable to exit a closed channel; i.e., blocker should become trapped. This idea is difficult to test in wild-type channels. For wild-type mHCN1, the kinetics of blocker dissociation and channel opening are too similar to be distin-

TABLE II

Gating Properties of Chimeras

	$V_{1/2}$	Slope	Increase of current with cAMP
	mV	*mV/e-fold change*	
mHCN1	−101.3 ± 0.3	−7.1 ± 0.2	−
H-S/P	−101.3 ± 0.3	−6.2 ± 0.3	−
H-S/S5	−113.2 ± 1.3	−10.8 ± 1.3	+
mHCN1-χ3	−82.8 ± 0.4	−8.1 ± 0.4	−
SPIH-χ3	−60.5 ± 0.8	−5.7 ± 0.7	+
SPIH	−73.5 ± 0.2	−5.4 ± 0.2	+

The values for SPIH, SPIH-χ3, and H-S/S5 were determined in the presence of 100 μM cAMP.

guished, while for wild-type SPIH, blockade is irreversible, making it impossible to measure dissociation. Fortunately, we could test for trapping using the triple mutant, SPIH-χ3. This mutant acquired completely reversible blockade like mHCN1, while preserving the fast activation of the parent channel SPIH.

To determine whether ZD7288 was trapped in this channel, we examined the rates for recovery from blockade using two different pulse protocols (Fig. 8). In each case, ZD7288 was applied for 1 s to achieve nearly complete blockade. In one case (Fig. 8, top), we observed recovery from blockade (τ = 3.1 s) after removing the blocker and keeping the voltage at −110 mV. In the other case (Fig. 8, bottom), when the blocker was removed, we immediately returned the voltage to +10 mV hoping to close the channels and trap the blocker. The voltage was held for 5 s at +10 mV. If the channels closed and trapped the blocker, there should be no recovery during this 5 s; if they do not, there should be substantial recovery. The voltage was stepped back to −110 mV to test whether recovery had occurred. There was no rapidly activated current, as would have been expected for unblocked (recovered) channels. The early current was completely blocked, and all of the current recovered at the normal rate, as though all of the channels remained blocked at the start of the pulse. Thus, no recovery had occurred during the 5-s step to +10 mV, showing that the blocker cannot exit from a closed channel.

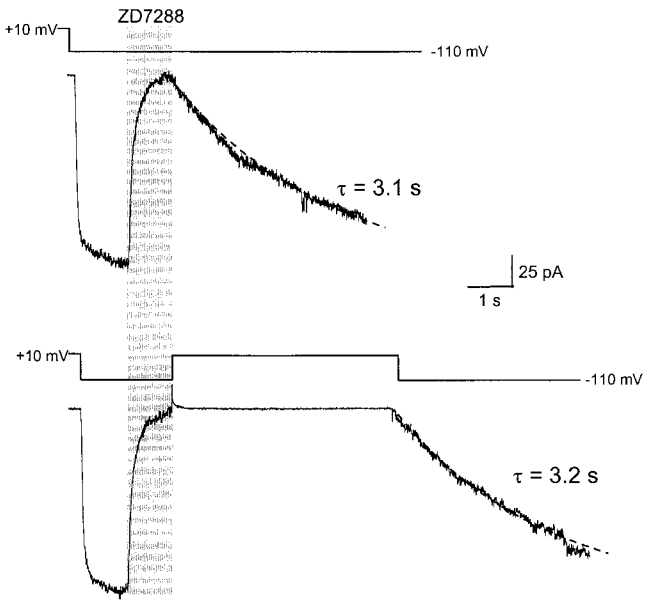

FIGURE 8. Trapping of ZD7288 in SPIH-χ3 mutant. (Top) 100 μM ZD7288 was applied to the excised inside-out patch at −110 mV for 1 s to achieve maximal blockade, and the blocker was removed to check the kinetics of blocker unbinding. The dashed line is a monoexponential fit to the slowly recovering current after removal of blocker (time constant = 3.1 s). (Bottom) 100 μM ZD7288 was applied to the same patch as shown above at −110 mV for 1 s to achieve complete block. The blocker was removed and, at the same time, the voltage was returned to +10 mV to close the channels. After 5 s, the voltage was stepped back to −110 mV to check recovery from the closed blocked state. The time constant for this recovery (3.2 s) was very similar to the value obtained above.

DISCUSSION

Voltage Dependence of ZD7288 Block

The most remarkable property of ZD7288 blockade of mHCN1 channels is its steep voltage dependence, corresponding to approximately four elementary charges moving through the entire transmembrane field. It has been previously demonstrated that the blocking effect of ZD7288 is relieved by hyperpolarization (BoSmith et al., 1993; Harris and Constanti, 1995; Gasparini and Di-Francesco, 1997) and that the voltage dependence of disinhibition was 4.8 mV/e-fold change (Berger et al., 1995). This slope value is equivalent to a zδ of 5.3 (similar to zδ ≈ 4.2 measured here for mHCN1).

This steep voltage dependence cannot be explained easily by intrinsic voltage dependence of the blocker, because the net charge of ZD7288 is only +1. In multi-ion channels, movement of the blocker in the pore can be coupled to the movement of permeant ions, leading to a higher voltage dependence (Hagiwara et al., 1976; Hille and Schwarz, 1978; Spassova and Lu, 1998). Although the permeation pathway of I_h channels may contain at least three ion binding sites (Frace et al., 1992; Wollmuth, 1995), the very high zδ for the relief of blockade still seems too high to be explained by this mechanism. On the other hand, the value for the voltage dependence of blockade agrees roughly with that of the gating process, with zδ ≈ 3.6. To account for the steep voltage dependence of ZD7288 blockade in terms of mHCN1 gating, we propose two possible models; one with preferential closed state block (but no direct binding to the closed state), and the other with two open states having different blocker affinities. The preferential closed state blockade model is suggested by the ob-

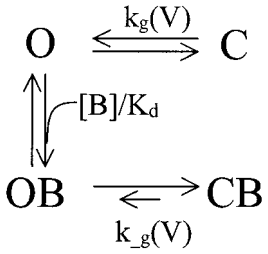

(SCHEME 1)

servations that the opening of the channel is required for the block and that the blocker can be trapped in closed state of the channel (Scheme 1). At the less hyperpolarized voltages, the blocker binds weakly to the open state, but the bound blocker favors closing and stable trapping of the blocker. Once the channel closes with the blocker bound inside the pore, reopening of the channel would be much more difficult than opening of the channel without blocker. However, at more negative voltages, the blocked channels are driven into the lower affinity open blocked state. Thus, the blocker effect appears to be less efficient at the more hyperpolarized voltages. Fig. 9 summarizes our data for voltage-dependent block of mHCN1; the solid lines are provided by fits to this model with preferential closed state blockade. The midpoint ($V_{1/2}$) of the OB ↔ CB transition was −130 mV, which is ~20 mV more negative than the $V_{1/2}$ (−112 mV) of the O ↔ C transition, i.e., binding of the blocker stabilizes the closed state.

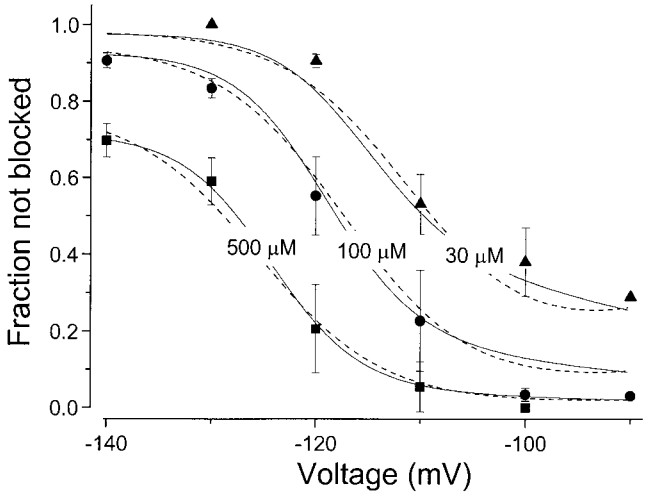

FIGURE 9. Voltage dependence of the ZD7288 block predicted by two possible models. A fraction of the current not blocked at different voltages was measured at three different concentrations of ZD7288 (30, 100, and 500 μM). The solid lines are the fits with the preferential closed state block model (Scheme 2), where k_g = exp[−(V − 111.8)/4.9], k_{-g}= exp[−(V − 129.6) / 4.3], and K_d = 1257.6 μM. The dashed lines show the fit using the two open state model (Scheme 2), where k_g = exp[−(V − 95.6)/15.0], k_t = exp[−(V − 97.5)/6.0], K_{d1} = 6.0 μM and K_{d2} = 1799.7 μM.

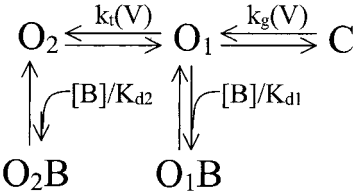

(SCHEME 2)

Another possible model with a similar behavior has multiple open states with different affinities for the blocker (Scheme 2). We assume that there are two open states (of similar conductance) with voltage-dependent switching between them; both states are blocked by ZD7288 but with different affinities. Opening of the channels by hyperpolarization allows ZD7288 to bind with a high affinity to the O_1 state. However, further hyperpolarization drives mHCN1 channels to another open state (O_2), and this conformational change either prevents ZD7288 from binding or reduces its affinity substantially. Thus, blocker potency decreases at more hyperpolarized voltages. The dashed lines in Fig. 9 indicate the fits according to this model with two open states, where O_1 binds blocker with a K_d of 6.4 μM and O_2 has much lower affinity (K_d = 1.3 mM).

Both models can mimic the experimental observations, but it is difficult to decide between them. Our observation of blocker trapping demands some form of closed state blockade; on the other hand, prominent delays in deactivation kinetics provide a clear indication of multiple open states (our unpublished observation). The correct description will probably incorporate features of both models.

Blockers that appear to bind in the pore but have a closed state preference have been described for other channels. High affinity binding of tetracaine to cyclic nucleotide–gated channels occurs only with the closed conformation of the pore (Fodor et al., 1997). In *Shaker*, Kv2.1 and Kv3.1, 4-aminopyridine (4-AP) preferentially enters and blocks the activated channel. Once bound, 4-AP can be trapped by closing of the channel, such that the blocker accumulates in closed channels and slowly dissociates from open channels (Kirsch and Drewe, 1993; McCormack et al., 1994). Thus, blocker potency increases in the closed state of the channel.

Comparison with Previous Observations

Previous work suggested that I_h blockade by ZD7288 does not require prior opening of channels. The different result seen here may be simply a difference in the variety of the h-channel studied, or it may be because of different experimental conditions. All previous experiments on ZD7288 blockade were done in a whole-cell mode with continuous application of blocker, and it took a long time (minutes to tens of minutes) to achieve blockade (BoSmith et al., 1993; Harris and Constanti, 1995; Gasparini and DiFrancesco, 1997; Luthi et al.,

1998; Satoh and Yamada, 2000). Even extremely slow binding of blocker to closed channels could therefore produce a lack of use dependence in those experiments. The experiments in the present study were done with inside-out patches and brief application of ZD7288 using a solenoid valve, so that the blocker concentration and exposure time could be accurately controlled.

It is possible that the results showing non–use-dependent block of ZD7288 in the previous experiments were due to slow access of the blocker to the closed channel via a hydrophobic pathway (Hille, 1977; Harris and Constanti, 1995). Alternatively, even though most channels were closed at the holding voltage, a very small likelihood of opening may have allowed the blocker to equilibrate with its site over the long duration of the blocker application. Regardless of the reason for the discrepancy, our experiments clearly show that entry of the blocker into closed channels, if it occurs at all, must be much slower than the blockade of open channels. Fig. 3 C shows that onset of blockade is negligible at −70 mV, with most channels closed (at least 10-fold slower than in the open state). Fig. 5 D shows that, at −60 mV, the onset of blockade is reduced in proportion to the number of channels open, so that entry to closed channels must be at least 20-fold slower. Reducing SPIH open probability by removing cAMP also appears to prevent blocker binding: the onset of blockade with <5% activation (without cAMP) was ~20 times slower than with maximal activation (with 100 μM cAMP).

Previous observations on other blockers of I_h channels such as UL-FS 49 and DK-AH 268 have shown use-dependent onset of blockade (Van Bogaert et al., 1990; DiFrancesco, 1994; Janigro et al., 1997; Raes et al., 1998) together with relief of blockade with hyperpolarization. Our experiments on ZD7288 blockade suggest that the differences between ZD7288 and these other blockers are quantitative rather than qualitative.

The Site of ZD7288 Blockade

The characteristics of ZD7288 blockade appear to be compatible with binding of the compound in the pore. The blocker enters mainly or exclusively when the channel is open, and can be trapped in a closed channel. Moreover, substantial changes in blockade can be produced by mutations in S6, which is known from work on the related potassium channels to contribute to the pore (Doyle et al., 1998; for review see Yellen, 1998). The S6 mutations may indicate sites directly involved in binding, or they may produce global or local structural changes that alter the binding of the compound.

If the three S6 residues swapped between mHCN1 and SPIH are indeed critical for direct binding, then hydrophobic interaction may dominate the binding of the blocker to the channel. The combined mutations F456Y, L458M, and I460V in SPIH make the channel less hydrophobic, and these eliminate irreversible block by ZD7288. Remarkably, the inverse mutations in mHCN1 are sufficient to confer irreversible blocker binding. The strong effect of these mutations is partly explained because each mutation is present in all four subunits of the channel (assuming that like its molecular relatives, the functional I_h channel is a tetramer). Although the individual exchange mutations were not tolerated, we have found that substitution of cysteine at one of the three positions (SPIH 460, corresponding to *Shaker* position 474, facing the pore) is sufficient to allow completely reversible blockade of SPIH (data not shown).

Although there are indications of ZD7288 trapping in mHCN1 and SPIH, detailed experiments were prohibited either by slow activation of mHCN1 or by irreversible blockade of SPIH. The SPIH-χ3 mutant acquired completely reversible blockade like mHCN1, while preserving the fast activation of its parent SPIH. The clear-cut distinction between opening and unblock made it easy to observe trapping in this mutant. Trapping of blocker in channels was first proposed for quaternary ammonium compounds in the potassium channels of squid giant axon (Armstrong, 1971). Trapping has been also described for TEA, decyltriethylammonium (C_{10}; Holmgren et al., 1997), and 4-AP (McCormack et al., 1994) in *Shaker* voltage-dependent K^+ channels. The observations of trapping supported the idea that the pore of these channels contains a relatively large water-filled cavity, situated between the selectivity filter and activation gate and lined by hydrophobic residues (Armstrong, 1969, 1971). Trapping is supposed to occur by the closure of the activation gate when a blocker is inside the vestibule.

If ZD7288 indeed binds in the section of the pore lined by this part of S6, the behavior of the blocker suggests that the I_h activation gate may reside in the region below these residues (i.e., more intracellular). Of course, ZD7288 is much larger than the permeant ions Na^+ and K^+, so it remains possible that such an intracellular gate regulates access of the blocker, while another gate (e.g., in the selectivity filter) regulates ion flow. The three S6 residues identified here are located in a homologous position to the water-filled cavity of the KcsA channel (KcsA positions 103, 105, and 107; Doyle et al., 1998). They also correspond to positions 470, 472, and 474 of *Shaker* K_v channels. In *Shaker* channels, access of cysteine-modifying reagents or Cd^{2+} ions to 470C and 474C side chains is governed by the intracellular gate (Liu et al., 1997). Also, the 470C mutation affects the ability of *Shaker* channels to trap blockers (Holmgren et al., 1997). Recently, it was found that the equivalent positions of HERG channels (positions 652 and 656) contribute to a high affinity MK-499 binding site (Mitcheson et al., 2000). The coincidence of mutations critical for ZD7288 blockade with cavity positions

in KcsA, *Shaker*, and HERG, together with the observation of blocker trapping by channel closure, strongly suggests that I_h channels have an activation gate homologous to the intracellular activation gate of K_v channels. Why it opens with hyperpolarization rather than depolarization remains to be explained.

We thank Drs. U. Benjamin Kaupp and Gareth Tibbs for sharing their clones with us. We also thank Dr. Bruce Bean for helpful comments on the manuscript, members of our lab for discussion, and Tara Ogren and Tanya Abramson for transfected cells.

This work was supported by grants to G. Yellen from the National Institutes of Health (HL57383) and the McKnight Endowment Fund for Neuroscience.

Submitted: 2 November 2000
Revised: 5 December 2000
Accepted: 5 December 2000

REFERENCES

Armstrong, C.M. 1969. Inactivation of the potassium conductance and related phenomena caused by quaternary ammonium ion injection in squid axons. *J. Gen. Physiol.* 54:553–575.

Armstrong, C.M. 1971. Interaction of tetraethylammonium ion derivatives with the potassium channels of giant axon. *J. Gen. Physiol.* 58:413–437.

Ausubel, F.M., R. Brent, R.E. Kingston, D.D. Moore, J.G. Seidman, J.A. Smith, and K. Struhl. 1996. Current Protocols in Molecular Biology. John Wiley & Sons Inc., New York. Section 8.5.

Berger, F., U. Borchard, R. Gelhaar, D. Hafner, and T.M. Weis. 1995. Inhibition of pacemaker current by the bradycardic agent ZD 7288 is lost use-dependently in sheep cardiac Purkinje fibres. *Naunyn-Schmiedeberg's Arch. Pharmacol.* 353:64–72.

BoSmith, R.E., I. Briggs, and N.C. Sturgess. 1993. Inhibitory action of ZENECA ZD 7288 on whole-cell hyperpolarization activated inward current (I_f) in guinea-pig dissociated sinoatrial node cells. *Br. J. Pharmacol.* 110:343–349.

Brown, H., and D. DiFrancesco. 1980. Voltage-clamp investigations of membrane currents underlying pace-maker activity in rabbit sinoatrial node. *J. Physiol.* 308:331–351.

Brown, H.F., D. DiFrancesco, and S.J. Noble. 1979. How does adrenaline accelerate the heart? *Nature.* 280:235–236.

DiFrancesco, D. 1981. A new interpretation of the pace-maker current in calf Purkinje fibres. *J. Physiol.* 413:359–376.

DiFrancesco, D. 1986. Characterization of single pacemaker channels in cardiac sino-atrial node cells. *Nature.* 324:470–473.

DiFrancesco, D. 1993. Pacemaker mechanisms in cardiac tissue. *Annu. Rev. Physiol.* 55:455–472.

DiFrancesco, D. 1994. Some properties of the UL-FS 49 block of the hyperpolarization-activated (i_f) in sino-atrial node myocyte. *Pflügers Arch.* 427:64–70.

DiFrancesco, D., and P. Tortora. 1991. Direct activation of cardiac pacemaker channels by intracellular cyclic AMP. *Nature.* 351:145–147.

Doyle, D.A., J. Morais Cabral, R.A. Pfuetzner, A. Kuo, J.M. Gulbis, S.L. Cohen, B.T. Chait, and R. MacKinnon. 1998. The structure of the potassium channel: molecular basis of K^+ conduction and selectivity. *Science.* 280:69–77

Fodor, A.A., K.D. Black, and W.N. Zagotta. 1997. Tetracaine reports a conformational change in the pore of cyclic nucleotide–gated channels. *J. Gen. Physiol.* 110:591–600.

Frace, A.M., F. Maruoka, and A. Noma. 1992. External K^+ increases Na^+ conductance of the hyperpolarization-activated current in rabbit cardiac pacemaker cells. *Pflügers Arch.* 421:97–99.

Gasparini, S., and D. DiFrancesco. 1997. Action of the hyperpolarization-activated current (I_h) blocker ZD7288 in hippocampal CA1 neurons. *Pflügers Arch.* 435:99–106.

Gauss, R., R. Seifert, and U.B. Kaupp. 1998. Molecular identification of a hyperpolarization-activated channel in sea urchin sperm. *Nature.* 393:583–587.

Hagiwara, S., S. Miyazaki, and N.P. Rosenthal. 1976. Potassium current and effect of cesium on this current during anomalous rectification of the egg cell membrane of a starfish. *J. Gen. Physiol.* 67: 621–638.

Hamill, O.P., A. Marty, E. Neher, B. Sakmann, and F.J. Sigworth. 1981. Improved patch clamp techniques for high resolution current recording from cells and cell-free membrane patches. *Pflügers Arch.* 391:85–100.

Harris, N.C., and A. Constanti. 1995. Mechanism of block by ZD 7288 of the hyperpolarization-activated inward rectifying current in guinea pig substantia nigra neurons in vitro. *J. Neurophysiol.* 74: 2366–2378.

Hille, B. 1977. Local anesthetics: hydrophilic and hydrophobic pathways for the drug-receptor interaction. *J. Gen. Physiol.* 69: 497–515.

Hille, B., and W. Schwarz. 1978. Potassium channels as multi-ion single-file pores. *J. Gen. Physiol.* 72:159–162.

Holmgren, M., P.L. Smith, and G. Yellen. 1997. Trapping of organic blockers by closing of voltage-dependent K^+ channels: evidence for a trap door mechanism of activation gating. *J. Gen. Physiol.* 109:527–535.

Ishii, T.M., M. Takano, L.H. Xie, A. Noma, and H. Ohmori. 1999. Molecular characterization of the hyperpolarization-activated cation channel in rabbit heart sinoatrial node. *J. Biol. Chem.* 274: 12835-12839.

Janigro, D., M.E. Martenson, and T.K. Baumann. 1997. Preferential inhibition of I_h in rat trigeminal ganglion neurons by an organic blocker. *J. Membr. Biol.* 160:101–109.

Jurman, M.E., L.M. Boland, Y. Liu, and G. Yellen. 1994. Visual identification of individual transfected cells for electrophysiology using antibody-coated beads. *Biotechniques.* 17:876–881.

Kirsch, G.E., and J.A. Drewe. 1993. Gating-dependent mechanism of 4-aminopyridine block in two related potassium channels. *J. Gen. Physiol.* 102:797–816.

Liu, Y., M. Holmgren, M.E. Jurman, and G. Yellen. 1997. Gated access to the pore of a voltage-dependent K^+ channel. *Neuron.* 19: 175–184.

Ludwig, A., X. Zong, M. Jeglitsch, F. Hoffmann, and M. Biel. 1998. A family of hyperpolarization-activated mammalian cation channels. *Nature.* 393:587–591.

Ludwig, A., X. Zong, M.J. Stieber, R. Hullin, F. Hoffmann, and M. Biel. 1999. Two pacemaker channels from human heart with profoundly different activation kinetics. *EMBO (Eur. Mol. Biol. Organ.) J.* 18:2323–2329.

Luthi, A., T. Bal, and D.A. McCormick. 1998. Periodicity of thalamic spindle waves is abolished by ZD7288, a blocker of I_h. *J. Neurophysiol.* 79:3284–3289.

Maccaferri, G., and C.J. McBain. 1996. The hyperpolarization-activated current (I_h) and its contribution to pacemaker activity in rat CA1 hippocampal stratum oriens-alveus interneurones. *J. Physiol.* 497:119–130.

Mayer, M.L., and G.L. Westbrook. 1983. A voltage-clamp analysis of inward (anomalous) rectification in mouse spinal sensory ganglion neurones. *J. Physiol.* 340:19–45.

McCormack, K., W.J. Joiner, and S.H. Heinemann. 1994. A characterization of the activating structural rearrangements in voltage-dependent *Shaker* K^+ channels. *Neuron.* 12:301–315.

McCormick, D.A., and T. Bal. 1997. Sleep and arousal: thalamocortical mechanisms. *Annu. Rev. Neurosci.* 20:185–215.

Mitcheson, J.A., J. Chen, M. Lin, C. Culberson, and M.C. Sanguinetti. 2000. A structural basis for drug-induced long QT syndrome. *Proc. Natl. Acad. Sci. USA*. 97:12329–12333.

Pape, H.C. 1996. Queer current and pacemaker: the hyperpolarization-activated cation current in neurons. *Annu. Rev. Physiol.* 58: 299–327.

Pape, H.C., and D.A. McCormick. 1989. Noradrenaline and serotonin selectively modulate thalamic burst firing by enhancing a hyperpolarization-activated cation current. *Nature*. 340:715–718.

Raes, A., G. van de Vijver, M. Goethals, and P.P. van Bogaert. 1998. Use-dependent block of I_h in mouse dorsal root ganglion neurons by sinus node inhibitors. *Br. J. Pharmcol.* 125:741–750.

Santoro, B., D.T. Liu, H. Yao, D. Bartsch, E.R. Kandel, S.A. Siegelbaum, and G.R. Tibbs. 1998. Identification of a gene encoding a hyperpolarization-activated pacemaker channel of brain. *Cell.* 93: 717–729.

Santoro, B., S.G. Grant, D. Bartsch, and E.R. Kandel. 1997. Interactive cloning with the SH3 domain of N-src identifies a new brain specific ion channel protein, with homology to eag and cyclic nucleotide-gated channels. *Proc. Natl Acad. Sci. USA*. 94:14815–14820.

Santoro, B., S. Shan, A. Luthi, P. Pavlidis, G.P. Shumyatsky, G.R. Tibbs, and S.A. Siegelbaum. 2000. Molecular and functional heterogeneity of hyperpolarization-activated pacemaker channels in the mouse CNS. *J. Neurosci.* 20:5264–5275.

Satoh, T., and M. Yamada. 2000. A bradycardic agent ZD7288 blocks the hyperpolarization-activated current (I_h) in retinal rod photoreceptors. *Neuropharmacol.* 39:1284–1291.

Seed, B., and A. Aruffo. 1987. Molecular cloning of the CD2 antigen, the T-cell erythrocyte receptor, by a rapid immunoselection procedure. *Proc. Natl. Acad. Sci. USA*. 84:3365–3369.

Seifert, R., A. Scholten, R. Gauss, A. Mincheva, P. Lichter, and U.B. Kaupp. 1999. Molecular characterization of a slowly gating human hyperpolarization-activated channel predominantly expressed in thalamus, heart, and testis. *Proc. Natl Acad. Sci. USA*. 96:9391–9396.

Spassova, M., and Z. Lu. 1998. Coupled ion movement underlies rectification in an inward-rectifier K^+ channel. *J. Gen. Physiol.* 112: 211–221.

Strata, F., M. Atzori, M. Molnar, G. Ugolini, F. Tempia, and E. Cherubini. 1997. A pacemaker current in dye-coupled hilar interneurons contributes to the generation of giant GABAergic potentials in developing hippocampus. *J. Neurosci.* 17:1435–1446.

Van Bogaert, P.P., M. Goethals, and C. Simoens. 1990. Use- and frequency-dependent blockade by UL-FS 49 of the I_f pacemaker current in sheep cardiac purkinje fibres. *Eur. J. Pharmacol.* 187: 241–256.

Williams, S.R., J.P. Turner, S.W. Hughes, and V. Crunelli. 1997. On the nature of anomalous rectification in thalamocortical neurons of the cat ventrobasal thalamus in vitro. *J. Physiol.* 505:724–747.

Wollmuth, L.P. 1995. Multiple ion binding sites in I_h channels of rod photoreceptors from tiger salamanders. *Pflügers Arch.* 430: 34–43.

Yanagihara, K., and H. Irisawa. 1980. Inward current activated during hyperpolarization in the rabbit sinoatrial node cell. *Pflügers Arch.* 385:11–19.

Yellen, G. 1998. The moving parts of voltage-gated ion channels. *Q. Rev. Biophys.* 31:239–295.

Yu, H., F. Chang, and I.S. Cohen. 1993. Pacemaker current exists in ventricular myocytes. *Circ. Res.* 72:232–263.